LiDAR or Photogrammetry? Integration is the answer

LiDAR or Photogrammetry? Integration is the answer

Francesco Nex and Fulvio Rinaudo

Land Environment and Geo-ENgineering Department, LEGEND, Politecnico di Torino, C.so Duca degli Abruzzi 24, 10121, Torino. E-mail: francesco.nex@polito.it

Abstract

In the last few years, LiDAR and image-matching techniques have been employed in many application fields because of their quickness in point cloud generation. Nevertheless, the use of only one of these techniques is not sufficient to extract automatically reliable information.

In this paper, an integration approach of these techniques is proposed in order to overcome their individual weakness. The goal of this work is the automated extraction of man-made object outlines in order to reduce the human intervention during the data processing simplifying the work of the users. This approach has been implemented on both terrestrial and aerial applications, showing the reliability and the potentiality of this kind of integration.

Keywords: image matching, LiDAR, terrestrial, aerial, integration.

Introduction

The automated extraction of object geometries from laser scans and photogrammetric images has been a topic of research for decades. Both techniques offer the opportunity to collect reliable and dense 3D point data over objects or surfaces under consideration. In particular, soon after the laser scanner devices had been developed to a commercial level, many people speculated that photogrammetry would be totally replaced by laser scanners. On the other hand, other researches asserted that image matching techniques would be able to produce the same point clouds of LiDAR instruments without using expensive instruments. However, it has afterwards become more obvious that neither technique would assure complete and consistent results, in every operative condition.

LiDAR allows a direct and simple acquisition of positional information, collecting thousands of points per second and giving the possibility to acquire full waveform data. Nevertheless, this technique has non-negligible drawbacks due to the impossibility of directly obtaining radiometric and semantic information. Then, laser scanners are not able to give the exact position of the object breaklines [Cheng et al., 2004]. Still, LiDAR data has no redundancy, while the advantage of images is the similarity to human vision, well-known internal geometry, good interpretability and ability to capture texture and multichannel reflectance information [Rönnholm et al., 2007]. Anyway, image-matching techniques cannot assure to generate point clouds without blunders in every operative condition (especially in terrestrial ones). A mayor existing obstacle in the way of automation in photogrammetry is the complicated and sometimes unreliable matching procedure, especially when dealing with converging imagery with significant depth variations [Habib et al., 2004] or with

the presence of bad-textured areas. The Semi-Global Matching [Hirshmuller, 2008] has partially solved this kind of problems.
Both techniques request several automated and manual interventions, once the point cloud has been acquired, in order to extract the information of interest for the 3D model or drawing production: this work cannot be performed in a complete automatic way and, nowadays, this step represents the true bottleneck of the whole process. The segmentation and classification algorithms are not able to give affordable results in every operative condition: the need of an experienced user to complete processes, hours of work using complicated (and expensive) software and PC able to manage millions of points are usually requested. The same happens when drawings are requested: in these conditions, the plotting is manually performed, taking long time to achieve a complete product.
Many authors have suggested to face the weakness of these techniques and to improve the automation of their processing exploiting their complementary nature. Some papers consider this integration as a possibility of improving the produced point cloud [Alshawabkeh et al., 2004; Remondino et al., 2008] in terms of completeness and reliability. Other papers have described this integration considering it as a sharing of radiometric and ranging information in order to simplify the information extraction from laser scanner data. These works, however, only consider single images [Ardissone et al., 2007] and the extraction of information from data is performed manually, using only point cloud data. Other examples show tightly integration in terrestrial applications [Becker and Haala, 2007]. In these works, photogrammetry is employed to determine the position of littler details of the façade while the position of these details on the model is defined by LiDAR data. A similar approach, but applied to aerial cases, is described in [Cheng et al., 2008]. The first step of this approach is the LiDAR data segmentation by means of a region growing algorithm. Then, using this information, the extraction (guided by LiDAR data) of the buildings from images is performed. In McIntosh and Krupnik [2002], edges are detected and matched in aerial image stereo-pairs, refining the DSM produced by airborne laser scanner data and improving the representation of surface discontinuities, especially building walls or straight lines. The result of this approach is the generation of a TIN comprising the breakline information.
Starting from these works, a new integration approach is proposed in this paper: this approach is focused on the extraction of man-made manufacture outlines (building breaklines, roof outlines, etc.) both in terrestrial and aerial applications. LIDAR and photogrammetric techniques continuously share information during the whole processing in order to complete the image and the point cloud information. These techniques work independently and share information to perform these tasks in a more complete and reliable way, overcoming their individual limits and achieving better results than each technique separately. The final goal is to try satisfying the exigencies of the final users (photogrammetrists, surveyors, planners, designers, etc.) reducing the time of production of a drawing and limiting the manual intervention in post processing phases.
In the following, the potentiality and the reliability of this kind of integration will be shown in different applications.

The algorithm

The proposed algorithm tries to merge image matching and LiDAR data processing. The main idea of this process is quite simple: the reliable information of laser scanners are

used as approximate DSM in order to help the matching algorithms and, then, the obtained information are employed to speed up the drawing production or the point cloud segmentation and the modelling. Combining this information the individual weakness of each singular technique can be overcome, reaching a reliable result in almost all the operative conditions.

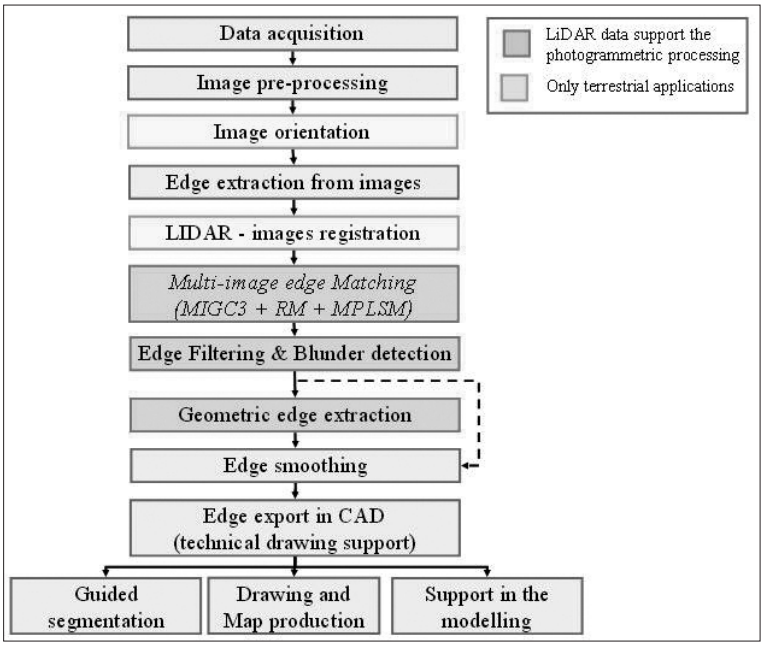

Figure 1 - Algorithm workflow.

The matching algorithm has been implemented considering a multi-image approach as these techniques allow an improvement to be made in geometric precision and reliability with respect to image pairs [Zhang, 2005]. The implemented algorithm, then, considers the epipolar geometry between images in order to reduce the search area in adjacent images, and thus decreasing the number of blunders to a great extent. The run on the epipolar line is further reduced by the approximate z-value that is provided by the LiDAR data. The extracted edges can be checked and improved using the LiDAR information in order to define the 3D geometric outlines of the surveyed objects. This kind of information can be used as rough drawing of the object or it can be used as additional information in the segmentation and modelling processes.
This approach has been initially implemented in terrestrial applications but it is then adapted to aerial cases, achieving good results in both these applications. The proposed algorithm can be divided into the following steps. A general workflow for both terrestrial and aerial applications is shown, in Figure 1.

Data acquisition

The data acquisition conditions the goodness of the achievable results: good image quality and a noiseless LiDAR acquisition can improve the results of the automated algorithms.

In the terrestrial acquisitions, several tests have shown that the images should be acquired according to two different configurations in order to achieve better results in the matching process: the *ad hoc* multi-image configuration [Nex and Rinaudo, 2009] and the sequence of converging images [Nex, 2010]. The central image of both configurations will be considered as reference image in the following matching process. In aerial acquisitions, high overlaps between images and adjacent strips are mandatory.
The LiDAR data, in terrestrial cases, is acquired close to the reference image position in order to have approximately the same occluded areas as the reference image. Median filtering reduces the noise of the LiDAR point cloud that usually affects the data.

Image pre-processing
In order to enhance the images, two different approaches are used considering two different topics: the edge extraction from the reference image and the matching process.
In order to improve the edge extraction, the reference image is previously processed using a non-linear Edge Preserving Smoothing (EPS) filter. In particular, the Sigma Filter [Lee, 1983] has been used: this algorithm is able to smooth the little radiometric variations preserving and enhancing the main edges on the image. The boundaries of the man-made objects on the image are sharpened and smoothed deleting the little radiometric changes that affect the surfaces of these elements. Therefore, the edge extraction allows the object boundaries to be extracted, neglecting the useless information. In general, the pre-processing allows number of detected edges to be increased respect to the original image [Nex, 2010].
On the opposite, the radiometric variations (texture) are of primary relevance in the matching process and they must be stressed to improve the results. For this reason, an Adaptive Gaussian Smoothing is performed in order to filter the image according to the noise level evaluated on the uniform areas of the image. Then, the image enhancement is achieved using a Wallis filter.

Image orientation (3 or more images)
In the aerial case, images and LiDAR data are already oriented in the same reference system. In terrestrial cases, the A^{2}SIFT (Auto-Adaptive Scale Invariant Feature Transform) operator [Lingua et al., 2009] has been adopted in the tie-point extraction: for a detailed description of the algorithm, refer to [Lingua et al., 2009]. Then, a robust relative orientation (Least Median Square, LMS) is, performed in order to eliminate any mismatch [Lingua and Rinaudo, 2000].
The extracted tie points are merged together with the Ground Control Points (GCP) and a bundle block adjustment is performed. Images are oriented in a Photogrammetric Reference System (PRS) in order to have the z-coordinate normal to the main plane of the façade. Sub-pixel accuracy is requested in order to perform the following matching algorithms.

Edge extraction from reference image
The central image is chosen as reference image, as it has been already said. After that, the edge extraction is performed by the well-known Canny operator. The final goal is to define only some "dominant" points able to provide a quite good approximation of the edge trend for its reconstruction in the matching process. The dominant points are recorded and linked by straight edges [Nex, 2010].

The edges are only extracted in the regions of interest: i.e. façade glass, in terrestrial acquisitions, is always excluded as it could create mismatches and blunders due to reflection.

LIDAR data registration

In the aerial case, images and point clouds are usually registered in the same coordinate reference system. In contrast, the point cloud of terrestrial acquisitions is registered in the PRS by means of a spatial roto-translation. This step is made possible using the coordinates of the reflective markers that are both visible on the point cloud and the images. In this way, the information between the images and the point cloud are shared.

Edge matching between images

A multi-image matching algorithm has been set up. This process can be divided in three steps. The first algorithm is a modification of the Multi-Image Geometrically Constrained Cross Correlation MIGC^3 [Zhang, 2005]. Through this algorithm, the dominants points of each edge are matched in all the images in order to reconstruct the breakline positions in 3D. The images are preliminarily undistorted (using the camera calibration data) in order to ease them into a central perspective [Nex, 2010].

The MIGC^3 is able to match a high percentage of the extracted dominant point. Nevertheless, more than one reliable solution can be possible considering only the cross correlation values. A relational matching technique has been developed in order to solve these ambiguous matches and to improve the rate of the successfully matched points. This algorithm integrates the figural continuity constraint through a probability relaxation approach [Kittler and Hanhock, 1989; Christmas et al., 1995] and it is able to solve several ambiguities of the matching process. The method uses the already matched dominants points as "anchors" and defines, in an iterative way, the more suitable match between candidates imposing a smoothing constraint.

Finally, a Multi-Image Least Square Matching (MILSM) [Baltsavias, 1991] with the epipolar constraint has been performed for each extracted point to improve the accuracy up to a sub-pixel dimension. Considering an affine transformation between patches, the estimation of all these parameters is often ill-posed on the image patch of an edge. For this reason, the parameters are initially orthogonalised and the Student t-test is performed to determine their significance is evaluated excluding any undeterminable parameters [Gruen, 1984].

Edge filtering & blunder detection

Blunders are initially deleted from extracted edges using a filter that considers the reciprocal point positions on the same edge: the position of a point is "predicted" considering the neighbouring dominant points of the edge and then the difference between the predicted and real position of the point is evaluated. If the difference value is higher than a threshold, the point is deleted [Nex and Rinaudo, 2009]. This filter works well if the blunders are isolated from each other.

A second, more robust, filter can be used to correct the edges when several blunders are close together: this algorithm uses LiDAR data to verify the correctness of each dominant point: when it is farther than a threshold from the point cloud, the point is deleted (see Fig. 2).

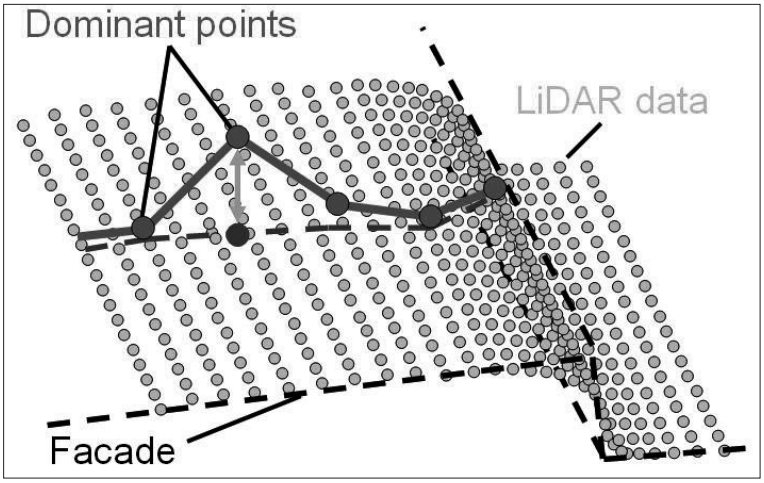

Figure 2 - Edge Filtering using the LiDAR information.

Geometric edge extraction

Image matching allows radiometric edges to be extracted. Most of these edges are due to shadows or radiometric changes but they have no geometric correspondence. Only geometric boundaries are of interest in surveying graphic drawings and modelling. For this reason, each dominant point on the extracted edges is considered with respect to the LiDAR point cloud and it is verified whether a geometric discontinuity occurs in the data close to the edge point. An edge breakline is detected considering the shape of the point cloud close to each dominant point. Few (4-6) neighbouring points (black points in Fig. 3) around the dominant point are considered, and the local curvature is evaluated. In general, curvatures will be high in at least one direction when a geometric discontinuity occurs. LiDAR point clouds usually smooth the geometric boundaries so a double check is performed evaluating the curvature between the neighbouring points and the dominant points (dark grey point in Fig. 3) and only LiDAR data using a correspondent point (the grey point in Fig. 3 instead of the dominant point) on the LiDAR data. In this way, two maximum curvature angles (α_1, α_2) are evaluated. Two different thresholds (T_1 and T_2, where $T_1 > T_2$) are set for each of them. When $\alpha_1 > T_1$ and $\alpha_2 > T_2$, a dominant point on a geometric edge has been detected. For a more detailed description refer to [Nex, 2010].

Edge smoothing

The edges extracted by the matching algorithm are random noise affected and they cannot be directly used in the drawing production or in the segmentation process. For this reason, a smoothing is needed in order to define a regular shape of the object, easing the edges in lines and curves. The great majority of edges in both close range and aerial applications can be classified in sets of lines and second order curves. Therefore, each edge must be split in different *basic entities* that describe its linear or curved parts separately: to do that, the changes in direction of the edge are considered [Nex, 2010]. Then, each separate *basic entity* is simplified in lines and curves. The line and the curve equations are fitted with a robust least square approach using the dominant point information. At first the linear

model is fitted: if the linear model gives high residuals, the second order curve model will be fitted. When the curve model does not correctly fit the data, the edge is re-processed splitting them in *sub-basic entities*. After the fitting of the entities, the whole edge is finally reconstructed by linking them together in a unique smoothed edge. The improvement given by the smoothing can be easily noticed in Figure 4, where several lines on a façade before (a) and after (b) the smoothing are considered.

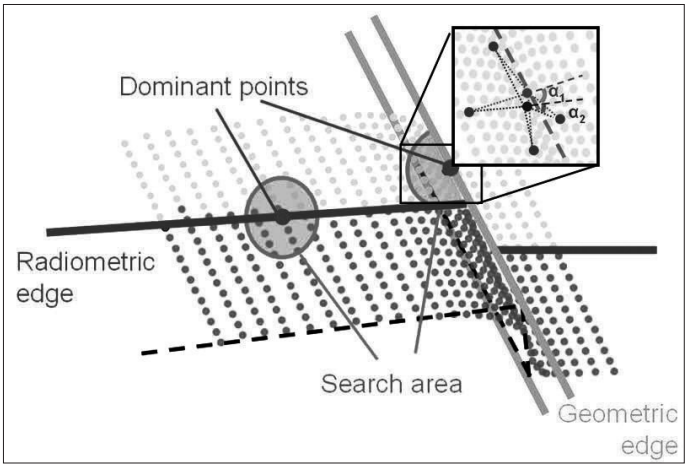

Figure 3 - Radiometric and Geometric edges and search area in the geometric filtering.

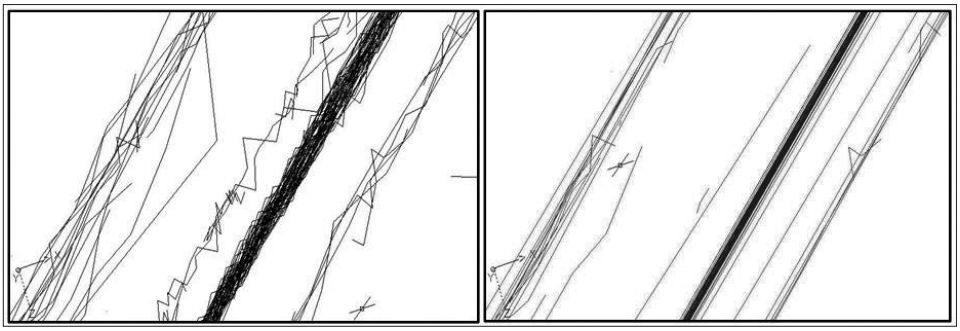

a) b)

Figure 4 - Difference in the noise level between the unsmoothed (a) and the smoothed data (b).

Export edges in CAD

Geometric edges are exported in CAD in order to give a good preliminary data for the graphic drawing realization of the survey or to be used as additional information in the segmentation and modelling process [Chiabrando et al., 2010].

The algorithm has been completely implemented in a *Matlab* code: the computation time has not been assessed during the performed tests.

Experimental tests

Several tests have been performed on both terrestrial and aerial applications: the main topic of these tests has been to show, on one hand, the geometric accuracy and, on the other hand, the effectiveness of the approach. The geometric accuracy assessment has been already discussed in [Nex and Rinaudo, 2009] and in [Lingua et al., 2010], where results comparable to manual restitution have been achieved.
In the following a brief summary of the results achieved is given: in particular, the examples of the achieved results on historical façades and on urban areas will be presented.

Valentino Royal Castle façade - Torino

The following test was performed on several parts of the Royal castle of Valentino (the Politecnico di Torino Architecture Faculty headquarter) in Torino. A point cloud of the court palace was acquired and several parts of the palace were considered in order to evaluate the performances of the algorithm in different conditions. The tests were performed using a *Riegl LMS-420* in the LiDAR acquisitions and a calibrated *Canon EOS-5D* in the image acquisitions.

Figure 5 - Reference image of the test, used in the multi-image matching process.

In particular, the "loggia" (Fig. 5) of the palace was analyzed acquiring seven images with a converging geometry. The taking distance was about 15 m. The 83% of the dominant points were successfully matched and only the 5% of these points were filtered during the blunder detection process.
The results achieved after this step are reported in Figure 6. The quality of the matched edges usually decreases in the parts of the façade tilted respect to the image planes. Then, the geometric filtering did not succeed in the complete deletion of the edges due to radiometric variations.

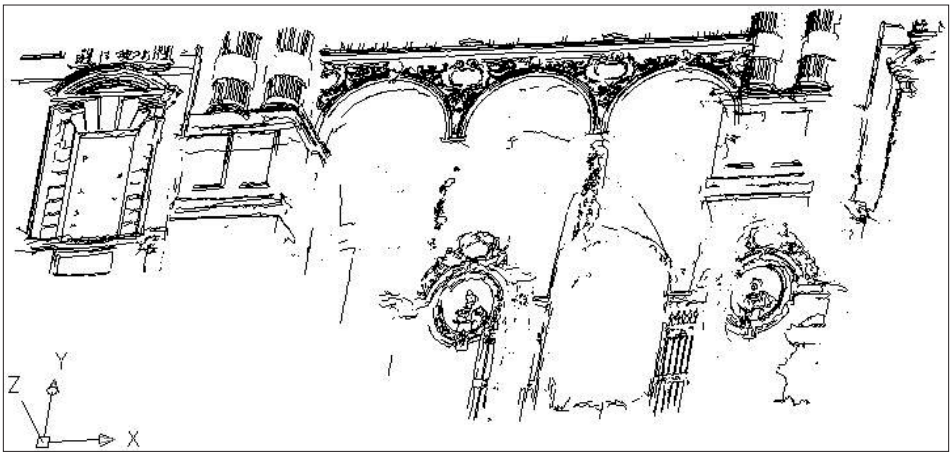

Figure 6 - Matched edges after the edge filtering and blunder deletion in the loggia test.

The smoothing was performed considering the complete set of edges (radiometric and geometric). The results were satisfying, especially if the complexity of the façade is considered (Fig. 7).

Figure 7 - Smoothed edges in the loggia test.

A second portion of the façade was a building corner. In this test, 5 images according to an *ad hoc* geometric configuration were acquired. As in the previous tests, glasses were deleted in order to avoid blunder generation during the matching process (Fig. 8).
The quality of the extracted edges was high in terms of completeness all over the image (see Fig. 8): 132412 dominant points were extracted in the analysed area. The 84% of these points were successfully matched, achieving a very good result. Then, only the blunder detection process (Fig. 9) deleted the 7% of the matched points.

Figure 8 - Extracted edges on the reference image in the corner test.

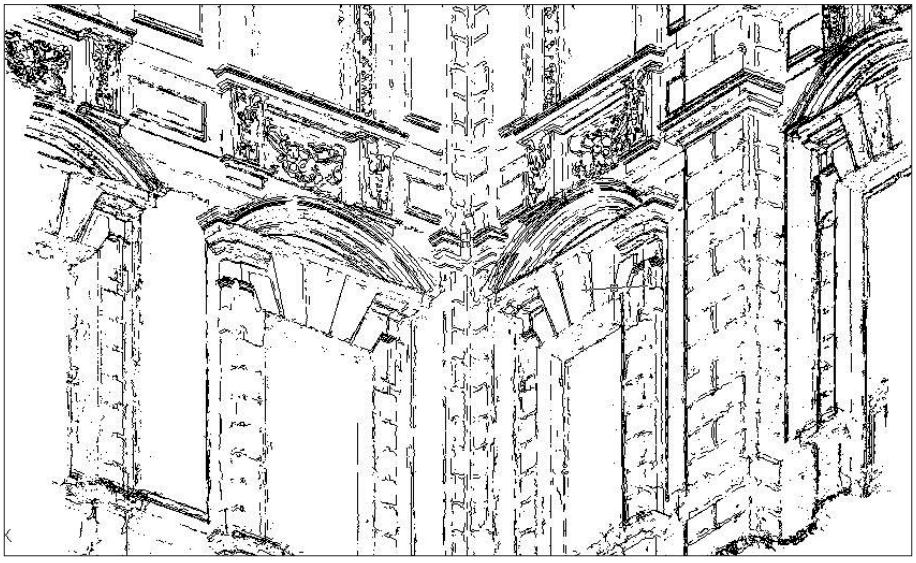

Figure 9 - Matched edges after the edge filtering and the blunder deletion.

The edges were filtered according to the geometric edge filtering. The results are very similar to the data before this step: only few shadows were removed, while some decorations were preserved because curvatures in correspondence of these details are very high.
Finally, the edge smoothing was performed. The results in Figure 10 show the effectiveness of this step in all the parts of the façade: the algorithm was able to automatically recognize the arcs from the lines and ease them in regular lines and second order curves.

Figure 10 - Smoothed edges in the corner test.

Urban area - Torino

A set of six images acquired from an Intergraph DMC camera (13824 x 7680 pixels) were available. These images were acquired with an overlap of about 60% in the flight direction. A Ground Sample Distance (GSD) of about 9 cm in the first strip and 11 cm in the second one was available because of the different flight height (about 100 m of difference). Luckily, this problem did not compromise the results of the proposed approach.

The DSM was created starting from a point cloud (2 pts/m^2) acquired by ALTM Gemini 167 kHz Optech instrument: only the first pulse was considered in the point cloud generation. Only patches of 3500 x 4000 pixels were extracted from the reference image and from the corresponding area on the other images. The extracted area considered a very dense urban area of the city.

The edge extraction succeeds in an almost complete description of the main outlines of the buildings, as shown in Figure 11: 185692 dominant points were extracted all over the analyzed area. Nevertheless, several edges were incomplete and the outline description was sometimes influenced by the radiometric variations of the roofs. In particular, several useless edges were detected in correspondence of shadows around radiometric variations on the roofs or in correspondence of vegetated areas.

The extracted edges were matched all over the image: the percentage of successfully matched points, on the whole area, was approximately 81%. This percentage is pretty high, especially if it is considered that the great part of unmatched points is concentrated in correspondence of wooded areas, roads and shadows. These points are rarely matched as their position changes during the image acquisition, in particular when the first strip images respect to the second strip (that was acquired several minutes later) are considered. On the contrary, more than the 95% of points in correspondence of the roofs outlines, also in presence of repetitive patterns, were correctly matched.

The extracted edges were filtered, according to the above-described approach. Thanks to this process, most of the blunders were correctly deleted. As it can be easily understood, most of these points are concentrated on the wooded areas, on the shadows and on the cars.

Figure 11 - Extracted edges on the reference image in the test area.

Then, the geometric filtering was performed on the edges in order to extract only the edges with a geometric correspondence. Nevertheless, this process does not succeed in the deletion of all the radiometric edges; the edges (due to shadow), close to the breaklines, were not cancelled by the filter (Fig. 12). The use of a denser point cloud did not appreciably improve the results, as the local curvature of the point cloud was still high in correspondence of these points and the algorithm was not able to filter the information in the correct way. In these conditions, a manual intervention was still required to complete the work.

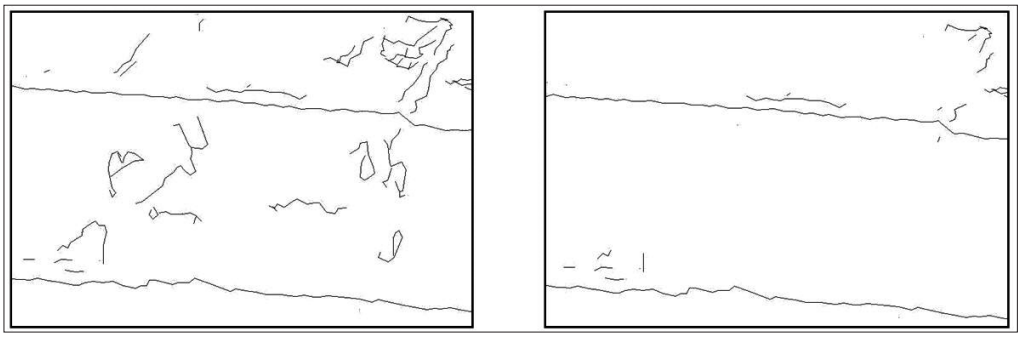

a) b)

Figure 12 - Edge before (a) and after (b) the geometric edge filtering in correspondence of a building.

Finally, the edge smoothing was realized in order to ease the noisy edges in lines and curves. Most of the edges were smoothed in a reliable way, as shown in Figure 13. Nevertheless, only a part of the buildings was completely described because of the incomplete edge extraction results.

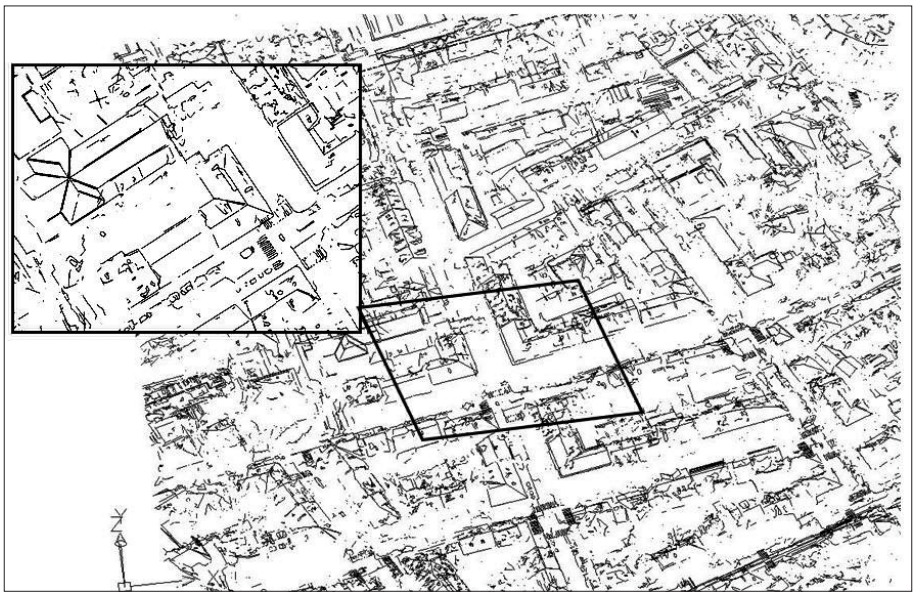

Figure 13 - Smoothed edges in 3D (edges before the geometric filtering).

Conclusion

A new integration approach between the LiDAR data processing and the multi-image techniques has been presented. The paper described the improvement this integration can give in comparison to each technique separately: the automation of the process has been increased while the manual intervention has been reduced to few operations in all the considered applications.

The data requested in the drawing production is automatically chosen as a "clever" selection of only useful data (lines in 3D). On planar surfaces, this method usually provides the necessary data to designers to complete the final drawing without any additional information (point clouds or topographic surveys). On curved surfaces, the extracted lines allow the decimation of the point cloud to be performed, defining the boundaries of each element of the façade.

The photogrammetric algorithms have been fully developed, as the matched edges are almost complete in every operative condition. The rate of points correctly matched is usually over 80% in both terrestrial and aerial applications. Then, the number of mismatches is reduced and they can be easily deleted by using the LiDAR information. In general, the results depend on the image-taking configuration: high overlaps and high number of images are recommended. The algorithm can achieve good results for repetitive patterns, particularly if more than three images are used. The number of mismatches is usually low and decreases

as the number of images increases.
On the contrary, several improvements are still requested to exploit the full potentiality of the method in the geometric filtering of the edges. Dense point clouds in the laser scanner acquisition are not strictly necessary during the matching process while they are instead requested in the filtering of geometric edges. The more the laser scanner data is dense the more the filtering is accurate; anyway, useless data are not successfully filtered and a manual intervention is still required.
Due to the complexity of the object to be described, the edge extraction is still the most critical step of the proposed approach. The edge extraction performed by an edge extractor sometimes does not succeed in the correct outlines determination as it is usually influenced by the presence of shadows or radiometric variations, especially in the aerial applications. This problem influences the goodness of the following steps of the workflow limiting the completeness of the result. The edge preserving smoothing algorithm can only reduce this problem, but it is not able to completely solve it. For this reason, several improvements in the edge extraction will be performed. In particular, the reliability of the image segmentation will be used to improve the building outlines determination: the goal of this study will be the automatic extraction of outlines only in correspondence of useful data.
In conclusion, this work showed the potentiality of this kind of integration, even if several improvements have to be performed. The possibility to use multi-echo point clouds and multi-spectral images will increase the automation in the extraction of useful information for the modelling and map production, extending this process to other elements, such as vegetation, and making possible new solutions and new applications.

References

Alshawabkeh Y., Haala N. (2004) - *Integration of digital photogrammetry and laser scanning for heritage documentation*. Proceedings of: XXI ISPRS Congress, Istanbul, Turkey.

Ardissone P., Bornaz L., Rinaudo F. (2007) - *3D Height Accuracy Survey and modeling for Cultural Heritage documentation and restoration*. In: VAST 2007 - Future technologies to empower heritage professionals, Brighton 26-30 November 2007.

Baltsavias E. (1991) - *Multiphoto Geometrically Constrained Matching*. Phd. dissertation, ETH Zurich, Switzerland. ISBN 3-906513-01-7.

Becker S., Haala N. (2007) - *Combined feature extraction for façade reconstruction*. In: ISPRS Workshop on Laser Scanning 2007 and SilviLaser 2007, Espoo, September 12-14, Finland.

Chiabrando F., Nex F., Piatti D., Rinaudo F. (2010) - *Integration between calibrated time-of-flight camera data and multi-image matching approach for architectural survey*. Proceedings of SPIE, The International Society For Optical Engineering, Vol. 7830: 1-12. ISSN: 0277-786X. doi: 10.1117/12.864971.

Christmas W. J., Kittler J., Petrou M. (1995) - *Structural Matching in Computer Vision Using Probabilistic Relaxation*. In: PAMI, Vol. 17, No. 8: 749-764.

Chen L.C., Teo T.A., Shao Y.C., Lai Y.C., Rau J.Y. (2004) - *Fusion of LIDAR data and optical imagery for building modeling*. Proceedings of: XXI ISPRS Congress, Istanbul, Turkey.

Cheng L., Gong J., Chen X., Han P. (2008) - *Building boundaries extraction from high*

resolution imagery and LiDAR data. In: International Archives of Photogrammetry, Remote Sensing and Spatial Information Science, Beijing, Vol. XXXVII, Part B3b.

Gruen, A. (1984) - *Data processing methods for amateur photographs*. Proceedings of: XVth International Congress of Photogrammetry and Remote Sensing, Rio de Janeiro, Brazil, June 1984.

Kittler J., Hancock E.R. (1989) - *Combining evidence in probabilistic relaxation*. Int. ’1 J. Pattern Recognition und Artificial Intelligence, vol. 3: 29-51. doi:10.1142/S021800148900005X

Habib A.F., Ghanma M.S., Tait M. (2004) - *Integration of LIDAR and photogrammetry for close range applications*. Proceedings of: XXI ISPRS Congress, Istanbul, Turkey.

Hirshmuller H. (2008) - *Stereo Processing by semiglogal matching and mutual information*. In: IEEE Transactions on pattern analysis and machine intelligence, Vol.30 N.2: 328-341. doi:10.1109/TPAMI.2007.1166

Lee J.S. (1983) - *Digital image smoothing and the sigma filter*. In: Comput. Vis., Graph., Image Process., vol. 24: 255-269. doi:10.1016/0734-189X(83)90047-6

Lingua A., Rinaudo F. (2000) - *Aerial triangulation data acquisition using a low cost digital photogrammetric system*. In: International Archives of Photogrammetry and Remote Sensing, Vol. XXXIII/B2: 449-454. ISSN: 0256-184.

Lingua A., Marenchino D., Nex F. (2009) - *Performance analysis of the SIFT operator for automatic feature extraction and matching in photogrammetric applications*. In: SENSORS, Vol. 9 (5): 3745-3766. ISSN: 1424-8220, DOI: 10.3390/s90503745.

Lingua A., Nex F., Rinaudo F. (2010) - *Integration of Airborne Laser Scanner and multi-image techniques for map production*. Proceedings of SPIE Remote Sensing, Vol. 7831: 1-14. ISSN: 0277-786X.

McInotsh K., Krupnik A. (2002) - *Integration of laser-derived DSMs and matched image edges for generating an accurate surface model*. In: ISPRS Journal of Photogrammetry and Remote Sens*ing*, Vol. 56, Issue 3: 167-176. doi:10.1016/S0924-2716(02)00042-4

Nex F. (2010) - *Multi-Image Matching and LiDAR data new integration approach*. PhD Thesis, Politicnico di Torino, Torino, April 2010.

Nex F., Rinaudo F. (2009) - *New integration approach of Photogrammetric and LIDAR techniques for architectural surveys*. In: Laserscanning 2009, Paris, 1-2 September.

Remondino F., El-Hakim S., Voltolini F. (2008) - *Integrating Techniques for Detail and Photo-Realistic 3D Modelling of Castles*. In: GIM International, Vol.22 (3): 21-25.

Rönnholm P., Honkavaara E., Litkey P., Hyyppä H., Hyyppä J. (2007) - *Integration of laser scanning and photogrammetry*. Proceedings of: IAPRS 2007 Vol. XXXVI, Part 3/W52, Espoo, Finland, September 12-14.

Zhang L. (2005) - *Automatic Digital Surface Model (DSM) generation from linear array images*. Thesis Diss. ETH No. 16078, Technische Wissenschaften ETH Zurich, IGP Mitteilung, N. 90.

Received 14/01/2011, accepted 7/03/2011